Am J Cancer Res 2025;15(7):3245-3266
www.ajcr.us /ISSN:2156-6976/ajcr0166745

*Original Article*

# Transcriptomic validation and clinical translation of CCDC78 as a prognostic biomarker in colorectal cancer

Jiang Gong, Binsong Xia, Lei Qian, Yingchang Cai

*Department of Anal and Pelvic Floor Surgery, The Quzhou Affiliated Hospital of Wenzhou Medical University, Quzhou People's Hospital, Quzhou 324000, Zhejiang, China*

Received June 12, 2025; Accepted July 23, 2025; Epub July 25, 2025; Published July 30, 2025

**Abstract:** This study investigates CCDC78 as a potential prognostic biomarker in colorectal cancer (CRC), incorporating both clinical correlation and functional validation. Analysis of 135 paired tumor and adjacent tissues revealed significantly elevated CCDC78 expression in tumor tissues ($P<0.001$), and higher expression levels were associated with markedly lower 5-year survival rates ($P=0.001$). Time-dependent ROC curves demonstrated robust prognostic performance at 12, 36, and 60 months (AUCs of 0.85, 0.84, and 0.82, respectively). In vitro assays showed that CCDC78 overexpression significantly enhanced cell proliferation, migration, and invasion ($P<0.05$), whereas siRNA-mediated knockdown suppressed these phenotypes and increased apoptosis ($P<0.01$). Cox regression analyses identified CCDC78 as an independent prognostic factor ($P=0.02$). Notably, despite similar baseline expression across CRC cell lines, SW480 cells were more sensitive to knockdown, while HCT116 cells more strongly recapitulated the overexpression phenotype. TCGA pan-cancer analysis showed upregulated CCDC78 in various tumors, including CRC, adrenocortical carcinoma (ACC), bladder cancer (BLCA), and kidney renal clear cell carcinoma (KIRC), reinforcing its broad oncogenic relevance. Correlation analyses linked high CCDC78 expression to older age, poor tumor differentiation, advanced TNM stage, lymph node metastasis, and distant metastasis. Immune profiling revealed negative associations with 11 immune cell types but a positive correlation with NK CD56 bright cells. Gene set enrichment analysis (GSEA) implicated CCDC78 in interferon-JAK-STAT, RIG-I/NFκB, and WNT signaling pathways. Altogether, these findings suggest that CCDC78 promotes CRC progression through enhancing tumor cell aggressiveness and modulating the immune microenvironment, underscoring its potential as a prognostic biomarker and therapeutic target.

**Keywords:** Colorectal cancer, CCDC78, prognostic biomarker, immune microenvironment, GSEA, survival analysis

## Introduction

Colorectal cancer (CRC) is one of the most common malignancies globally, ranking highest in both incidence and mortality among digestive system cancers [1]. According to the World Health Organization (WHO), approximately 1.93 million new cases and 935,000 CRC-related deaths were reported worldwide in 2020, establishing CRC as a major public health concern [2]. Rising incidence rates, particularly in developing nations, are attributed to lifestyle modifications, dietary shifts, and population aging [3]. Despite advances in diagnosis and treatment, encompassing endoscopic screening, targeted therapeutics, and immunotherapy, early detection remains suboptimal [4]. Patients diagnosed at advanced stages continue to experience poor prognosis, with five-year survival rates below 50% in specific populations [5]. This clinical challenge underscores the urgent need for novel biomarkers to facilitate early diagnosis, prognostic stratification, and personalized therapeutic strategies.

CRC pathogenesis involves a multifaceted interplay of genetic, epigenetic, and environmental factors [6]. Aberrant gene expression, dysregulated signaling cascades, and tumor microenvironment alterations are critical in the tumor initiation and progression [7]. The advent of high-throughput sequencing has enabled comprehensive profiling of tumorigenesis-associated genes and their interaction with the microenvironment [8]. However, established biomarkers including carcinoembryonic antigen (CEA)

https://doi.org/10.62347/THYT9980

and carbohydrate antigen 19-9 (CA19-9) demonstrate limited sensitivity and specificity for early detection and prognostic evaluation [9]. Consequently, identifying novel molecular biomarkers with both prognostic and therapeutic relevance has become a research priority in CRC.

Coiled-Coil Domain Containing 78 (CCDC78) encodes a protein featuring coiled-coil motifs, which participate in cytoskeletal organization, signal transduction, and cellular differentiation [10]. These coiled-coil domains commonly mediate protein-protein interactions and play crucial roles in intracellular signaling networks [11]. Nevertheless, CCDC78 expression patterns, functional mechanisms, and prognostic implications in CRC remain largely unexplored. As an emerging candidate in cancer research, elevated CCDC78 expression may be associated with tumor invasiveness, metastatic potential, and adverse patient outcomes. Whether CCDC78 contributes to CRC progression through tumor microenvironment modulation, immune response regulation, or critical pathway activation remains unclear. Additionally, the relationship between CCDC78 and immune cell infiltration, along with potential immunotherapeutic roles, warrants systematic investigation. Therefore, a comprehensive analysis of CCDC78 expression characteristics, prognostic significance, and underlying molecular mechanisms may clarify its tumorigenic role and identify novel diagnostic and therapeutic targets.

This investigation aims to comprehensively evaluate the expression profiles, prognostic significance, and potential biological mechanisms of CCDC78 in CRC, thereby laying the theoretical foundations for clinical application as a biomarker. Our study addressed several key objectives: 1) to analyze CCDC78 expression across various cancer types using pan-cancer datasets to assess its universality and specificity in tumor biology; 2) to evaluate CCDC78's prognostic relevance in CRC patients using univariate and multivariate Cox regression analyses and Kaplan-Meier survival analyses; 3) to explore correlations between CCDC78 expression and clinical parameters, including age, tumor differentiation, tumor-node-metastasis (TNM) staging, lymph node metastasis, and distant metastasis; 4) to examine its involvement in immune regulation and signaling pathway activity through immune cell infiltration analysis and Gene Set Enrichment Analysis (GSEA).

## Methods and materials

### *Sample size calculation*

The required sample size was estimated based on the findings of Matsuyama et al. [12], which reported a hazard ratio (HR) of 2.23 for ITGBL1 in predicting overall survival (OS) and a 5-year mortality rate of 29%. Using the formula for sample size calculation ($n = \frac{(Z_{\alpha/2} + Z_{\beta})^2}{(log(HR)^2 \times P \times (1 - P))}$), with α=0.05 (Zα/2= 1.96), β=0.2 (Zβ=0.84), HR=2.23, and P=0.29, a minimum of 59 samples was required.

### *Sample collection*

Clinical data and tissue samples were obtained from 135 CRC patients treated at Quzhou People's Hospital between January 2017 and March 2020. All patients provided written informed consent prior to participation. The study protocol and sample collection procedures were reviewed and approved by the Ethics Committee of Quzhou People's Hospital.

Inclusion criteria: pathologically confirmed colorectal adenocarcinoma (colon or rectum); radical surgical resection performed with intraoperative collection of paired tumor and adjacent non-tumor tissues, which were immediately preserved for subsequent qRT-PCR analysis of CCDC78 expression; availability of complete TNM staging based on AJCC/UICC criteria; a minimum follow-up duration of 5 years; expected survival time exceeding 6 months; and age between 18 and 85 years. Exclusion criteria: presence of other concurrent malignancies; receipt of neoadjuvant chemotherapy or radiotherapy prior to surgery; severe cardiovascular, hepatic, or renal dysfunction; or unclear origin of distant metastases.

### *Data acquisition and analysis*

This investigation utilized The Cancer Genome Atlas (TCGA) and Gene Expression Omnibus (GEO) datasets to assess CCDC78 expression, prognostic significance, and potential molecular mechanisms in both pan-cancer and CRC contexts. TCGA data (https://portal.gdc.cancer.gov/), accessed in October 2024, encompassed RNA-sequencing (RNA-Seq) data in

fragments per kilobase of transcript per million mapped reads [FPKM] format and corresponding clinical information across 33 cancer types. Sample selection criteria included complete CCDC78 expression data, definitive pathological diagnosis, clinical staging documentation, and follow-up duration exceeding six months. This yielded approximately 10,000 samples, comprising 643 CRC cases (colon adenocarcinoma [COAD] and rectum adenocarcinoma [READ]). The GEO GSE30378 dataset, based on teh Affymetrix Human Genome U133 Plus 2.0 Array platform (https://www.ncbi.nlm.nih.gov/geo/), facilitated Gene Set Enrichment Analysis (GSEA) to investigate CCDC78-associated signaling pathways.

*GSEA analysis*

GSEA was conducted using GSEA software (version 4.3.2) based on GSE30378 dataset analysis. The c2.cp.kegg and c5.go gene sets were analyzed. A total of 1,000 permutations were conducted, with statistical significance thresholds defined as $P<0.05$ and false discovery rate (FDR) q-value <0.25.

*Clinical data collection*

Clinical and pathological data from 135 CRC patients who underwent radical surgery between January 2017 and March 2020 were retrieved from hospital electronic medical records. Collected parameters included age, sex, tumor differentiation grade, TNM staging (American Joint Committee on Cancer [AJCC]/Union for International Cancer Control [UICC] criteria), lymph node metastasis status, presence of distant metastasis, tumor diameter, anatomical location (left colon, right colon, sigmoid colon/rectum), KRAS mutation status, P53 mutation status, and Ki67 proliferation index. All data were independently verified by two trained personnel to ensure accuracy and completeness.

*qRT-PCR analysis*

qRT-PCR was used to assess CCDC78 expression levels in tumor and adjacent non-tumor tissues from all 135 CRC patients. Total RNA was extracted from liquid nitrogen-preserved tissues using the EasyPure® RNA Kit (TransGen Biotech, Beijing, China). RNA purity was evaluated using a NanoDrop 2000 spectrophotometer (Thermo Fisher Scientific, USA), with OD260/280 ratios ranging from 1.8 to 2.0. Complementary DNA (cDNA) was performed with 1 μg of total RNA using TransScript® All-in-One First-Strand cDNA Synthesis SuperMix (TransGen Biotech) at 42°C for 30 minutes and 85°C for 5 seconds.

qRT-PCR was performed on and Applied Biosystems 7500 system (Thermo Fisher Scientific, USA). Each 20 μL reactions contained: 10 μL TransStart® Top Green qPCR SuperMix, 0.5 μL forward primer (10 μM, 5'-CTTGGGAGACGGCCTAGTGG-3'), 0.5 μL reverse primer (10 μM, 5'-GCCTCAGGCGCTAAAAGCAG-3'), 2 μL cDNA, and 7 μL nuclease-free water. The expected amplicon size was 193 bp. Glyceraldehyde 3-phosphate dehydrogenase (GAPDH) served as an internal control (forward: 5'-GAGTCCACTGGCGTCTTCAC-3'; reverse: 5'-ATCTTGAGGCTGTTGTCATACTTCT-3'). Thermal cycling conditions included initial denaturation at 95°C for 3 minutes, followed by 40 cycles of 95°C for 15 seconds, 60°C for 30 seconds, and 72°C for 30 seconds, with fluorescence collection per cycle. Relative expression levels of CCDC78 were calculated using the $2^{(-\Delta\Delta Ct)}$ method, normalized to GAPDH. All reactions were performed in triplicate, and results were analyzed using ABI 7500 software (version 2.3).

*Follow-up protocol*

Five-year follow-up data for the 135 CRC patients were collected through March 2025, with documentation of survival status and time of death. Follow-up was conducted via electronic medical record reviews, telephone interviews, and outpatient consultations. During the first postoperative year, patients were monitored monthly for survival, recurrence, and metastasis. From the second to the fifth year, follow-up assessments were conducted quarterly in conjunction with outpatient evaluations.

*Outcome measures*

*Primary outcomes:* CCDC78 expression in CRC tissues was determined using qRT-PCR, and its association with five-year overall survival was assessed using Kaplan-Meier analysis. Univariate and multivariate Cox regression analyses were conducted to determine whether CCDC78 served as an independent prognostic indicator. Additionally, TCGA data were used to analyze CCDC78 expression across 33 cancer

types to evaluate its tumor-type specificity and pan-cancer relevance in CRC.

*Secondary outcomes:* Correlations between CCDC78 expression and clinicopathological characteristics (age, differentiation grade, TNM staging, lymph node metastasis, distant metastasis) were analyzed. Immune correlation analyses were performed using CIBERSORT to estimate 23 immune cell subsets, and Spearman correlation was applied to examine relationships with CCDC78 expression. GSEA was utilized to explore signaling pathways associated with elevated CCDC78 expression, including type I interferon-Janus kinase-signal transducer and activator of transcription [JAK-STAT] and wingless-related integration site [WNT] pathways. Stratified and regression analyses were conducted to evaluate CCDC78 prognostic significance across subgroups defined by age and TNM stage, and to explore potential interactions with other clinical variables.

*Cell line sources*

The human colorectal cancer cell lines SW480 and HCT-116 were obtained from the American Type Culture Collection (ATCC), while the normal human colonic epithelial cell line FHC was purchased from BeNa Culture Collection (China). All cell lines were cultured in in Roswell Park Memorial Institute (RPMI)-1640 medium containing 10% fetal bovine serum (FBS) and 1% penicillin-streptomycin, maintained at 37°C in a humidified incubator with 5% $CO_2$.

*Cell transfection*

Cell transfections were performed using Lipofectamine® 3000 reagent (Thermo Fisher Scientific, Catalog No. L3000008) following manufacturer protocols. For CCDC78 overexpression, cells were transfected with the pcDNA3.1-CCDC78 plasmid (overexpression group) or an empty vector (pcDNA3.1-NC, negative control group). CCDC78 knockdown was achieved using a specific siRNA (si-CCDC78 group), with a non-targeting siRNA used as the negative control (si-NC group). Cells were harvested 48 hours post-transfection for subsequent experiments.

*EdU assay*

Cell proliferation was assessed using EdU Cell Proliferation Detection Kit (RiboBio, Catalog No. C10310-1). Transfected cells were incubated with EdU solution for 4 hours, followed by staining per manufacturer instructions. EdU-positive cells were visualized and quantified using a Leica DMI8 fluorescence microscope. The proportion of EdU-positive cells was calculated to assess proliferative activity.

*Transwell assay*

Cell migration and invasion were assessed using Transwell chambers (Corning, Catalog No. 3422). Transfected HCT-116 cells in serum-free medium (50,000 cells/well) were seeded into the upper chambers. The lower chambers were filled with RPMI-1640 medium containing 10% FBS to serve as a chemoattractant. Following 24-hour incubation, migrated cells on the lower membrane surface were fixed and stained with crystal violet (Solarbio, Catalog No. G1010). Cells were then imaged and counted under a Leica DMI8 microscope.

*Wound healing assay*

Cells were seeded in 6-well plates (Corning, Catalog No. 3516) and cultured to approximately 90% confluence. A linear scratch was generated in the cell monolayer using a 10 μL pipette tip. Cells were then washed with phosphate-buffered saline (PBS) to remove debris and incubated in serum-free medium. Wound closure was monitored and imaged at 0, 12, and 24 hours. Migration velocity quantified by measuring wound area reduction using ImageJ software.

*Flow cytometry*

Apoptosis assessment utilized flow cytometry (BD Biosciences, FACSAria™ Fusion). Cell staining employed Annexin V-fluorescein isothiocyanate/propidium iodide (FITC/PI) Apoptosis Detection Kit (BD Biosciences, Catalog No. 556547) per manufacturer instructions. Flow cytometry detected early and late apoptosis, with FlowJo software analysis calculating apoptotic cell proportions.

*Western blot analysis*

Total cellular proteins were extracted using RIPA flysis buffer (Beyotime, Catalog No. P0013C), and protein concentration were determined using the BCA Protein Assay Kit (Beyotime, Catalog No. P0012). Equal amounts

of protein were separated by 10% sodium dodecyl sulfate-polyacrylamide gel electrophoresis (SDS-PAGE) and transferred onto polyvinylidene fluoride (PVDF) membranes (Millipore, Catalog No. IPVH00010). Membranes were blocked and incubated overnight at 4°C with the following primary antibodies: CCDC78 (1:1000, Abcam, Catalog No. ab124767), phosphorylated JAK1 (p-JAK1; 1:1000, Cell Signaling Technology, Catalog No. 3371S), p-JAK2 (1:1000, Cell Signaling Technology, Catalog No. 3776S), p-STAT1 (1:1000, Cell Signaling Technology, Catalog No. 14994S), and p-STAT3 (1:1000, Cell Signaling Technology, Catalog No. 9131S). After washing, membranes were incubated with Horseradish peroxidase (HRP)-conjugated secondary antibodies (1:2000, Cell Signaling Technology, Catalog No. 7074S) for 1 hour at room temperature. Protein bands were visualized using an enhanced chemiluminescence (ECL) detection kit (Thermo Fisher Scientific, Catalog No. 32209) and quantified using ImageJ software.

*Statistical analysis*

Statistical analyses were performed using SPSS 20.0 and R software (version 4.3.3). Categorical data were expressed as percentages and compared using the chi-square test. The normality of continuous data was assessed using the Kolmogorov-Smirnov test. Normally distributed data were presented as mean ± standard deviation (SD) and compared using independent-sample t-tests, while non-normally distributed data were compared using the Mann-Whitney U test. Survival analysis was conducted using Cox regression models, with univariate and multivariate analyses performed to estimate hazard ratios (HR) and 95% confidence intervals (CIs).

Differential gene expression analysis was conducted with DESeq2. Kaplan-Meier survival curves were generated using the *survival* and *survminer* R packages, statistical significance was assessed by the log-rank test ($P<0.05$). Time-dependent receiver operating characteristic (ROC) curves were plotted using the *pROC* package. Forest plot for Cox regression were created using *forestplot*. *ggplot2* was utilized for generating scatter and lollipop plots, and clusterProfiler was used for GSEA (1,000 permutations, $P<0.05$, FDR $q<0.25$), Correlation analysis was conducted using Spearman's rank correlation with visualization via the *corrplot* package. Statistical significance was established at $P<0.05$. Results were visualized employing forest plots, survival curves, ROC curves, lollipop plots, and scatter plots, as appropriate.

## Results

*CCDC78 expression in pan-cancer analysis*

Pan-cancer analysis was performed to assess CCDC78 expression across multiple cancer types, revealing significant differential expression between normal and tumor tissues. Notably, CCDC78 expression was significantly upregulated in tumor tissues of bladder urothelial carcinoma (BLCA), breast invasive carcinoma (BRCA), colon adenocarcinoma (COAD), esophageal carcinoma (ESCA), kidney renal clear cell carcinoma (KIRC), liver hepatocellular carcinoma (LIHC), rectal adenocarcinoma (READ), stomach adenocarcinoma (STAD), and uterine corpus endometrial carcinoma (UCEC) (all $P<0.001$).

Elevated tumor expression of CCDC78 was also observed in kidney chromophobe (KICH) and prostate adenocarcinoma (PRAD) ($P<0.01$), as well as in cervical squamous cell carcinoma (CESC), cholangiocarcinoma (CHOL), kidney renal papillary cell carcinoma (KIRP), pheochromocytoma and paraganglioma (PCPG), and thyroid carcinoma (THCA) ($P<0.05$).

Conversely, lung adenocarcinoma (LUAD) and lung squamous cell carcinoma (LUSC) demonstrated significantly lower CCDC78 expression in tumor tissues compared to normal tissues ($P<0.05$). No significant differences were observed in glioblastoma multiforme (GBM) and pancreatic adenocarcinoma (PAAD) ($P>0.05$). See **Figure 1**.

*Prognostic value of CCDC78 in pan-cancer analysis*

The prognostic significance of CCDC78 across various cancer types was evaluated using univariate Cox regression analysis, followed by Kaplan-Meier survival validation. Forest plot analysis showed that high CCDC78 expression was significantly associated with overall survival (OS) in adrenocortical carcinoma (ACC),

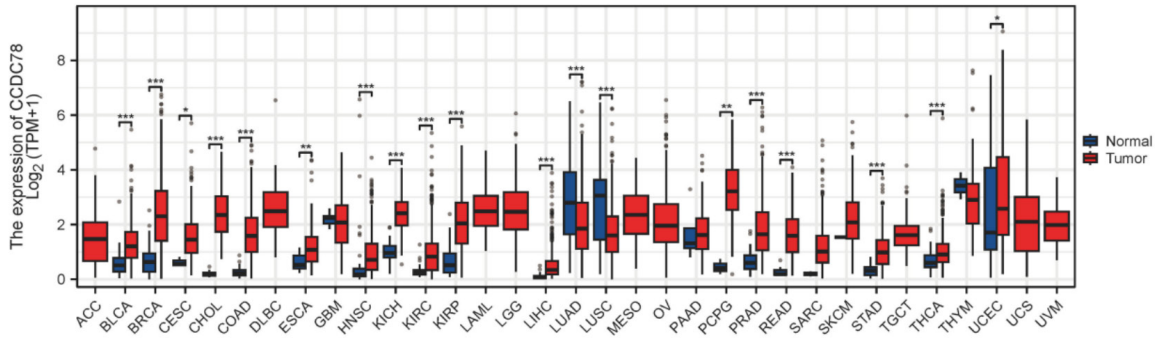


**Figure 1.** Differential expression of CCDC78 in pan-cancer analysis. Note: CCDC78, Coiled-coil domain containing 78; BLCA, Bladder Urothelial Carcinoma; BRCA, Breast Invasive Carcinoma; CESC, Cervical Squamous Cell Carcinoma; CHOL, Cholangiocarcinoma; COAD, Colon Adenocarcinoma; ESCA, Esophageal Carcinoma; GBM, Glioblastoma Multiforme; HNSC, Head and Neck Squamous Cell Carcinoma; KICH, Kidney Chromophobe; KIRC, Kidney Renal Clear Cell Carcinoma; KIRP, Kidney Renal Papillary Cell Carcinoma; LIHC, Liver Hepatocellular Carcinoma; LUAD, Lung Adenocarcinoma; LUSC, Lung Squamous Cell Carcinoma; PAAD, Pancreatic Adenocarcinoma; PCPG, Pheochromocytoma and Paraganglioma; PRAD, Prostate Adenocarcinoma; READ, Rectum Adenocarcinoma; STAD, Stomach Adenocarcinoma; THCA, Thyroid Carcinoma; UCEC, Uterine Corpus Endometrial Carcinoma.

BLCA, COAD, and KIRC (all P<0.05), but not in other cancer types (P>0.05, **Figure 2A**).

Kaplan-Meier survival analysis further confirmed that patients with elevated CCDC78 expression exhibited significantly shorter OS in ACC (**Figure 2B**), BLCA (**Figure 2C**), COAD (**Figure 2D**), and KIRC (**Figure 2E**), compared to those with low expression levels (P<0.05). These findings suggest elevated CCDC78 expression is associated with poor prognosis in select cancers, highlighting its potential utility as a cancer-specific prognostic biomarker.

*CCDC78 expression in CRC tissues and five-year survival association*

qRT-PCR analysis of tumor and adjacent normal tissues from 135 CRC patients revealed significantly higher CCDC78 expression in tumor tissues compared to adjacent non-tumor tissues (P<0.001, **Figure 3A**). Patients were stratified into high- and low-CCDC78 expression groups based on the optimal cutoff values determined by X-tile analysis. Kaplan-Meier survival analysis demonstrated that patients in high-expression group had significantly lower five-year survival rates compared to those in low-expression groups (P<0.001, **Figure 3B**). Time-dependent ROC analysis was performed to evaluate the prognostic accuracy of CCDC78 expression. The AUC values were 0.951 at postoperative 12 months, 0.935 at 36 months, and 0.743 at 60 months (**Figure 3C**), indicating robust short- to medium-term predictive performance, with moderate long-term prognostic value. Collectively, these findings suggest that high CCDC78 expression is strongly associated with unfavorable CRC patient prognosis, emphasizing its potential prognostic evaluation value.

*Association between CCDC78 expression and CRC clinicopathological features*

Analysis of CCDC78 expression in relation to CRC clinicopathological features revealed significant differences between high- and low-expression groups across multiple variables. Elevated CCDC78 expression was significantly correlated with advanced age (P<0.001), poor tumor differentiation (P=0.026), advanced TNM staging (P=0.001), presence of lymph node metastasis (P=0.006), and distant metastasis (P=0.002). These associations suggest high CCDC78 expression is linked to more aggressive tumor phenotypes. In contrast, no significant associations were observed between CCDC78 expression and gender, perineural invasion, tumor diameter, anatomical location, KRAS mutation status, P53 mutation status, or Ki67 proliferation index (P>0.05) (**Table 1**).

*CCDC78 expression across clinicopathological feature subgroups*

Further subgroup analysis demonstrated consistent trends in CCDC78 expression across key clinicopathological variables. Patients aged >65 years exhibited significantly higher

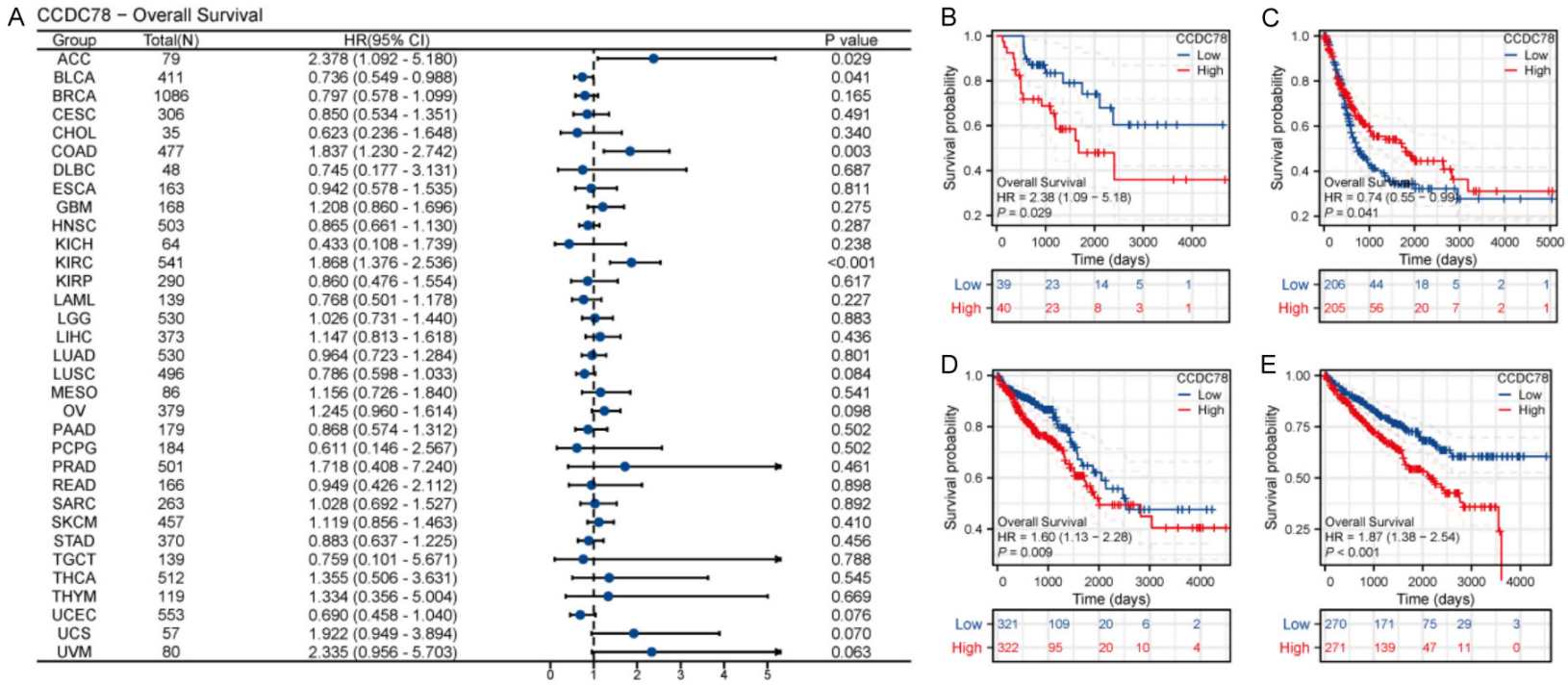


**Figure 2.** Prognostic value of CCDC78 in pan-cancer analysis. A: Univariate Cox regression forest plot of CCDC78 in pan-cancer. B: OS curves for ACC patients stratified by high- or low-CCDC78 expression. C: OS curves for BLCA patients stratified by high- or low-CCDC78 expression. D: OS curves for COAD patients stratified by high- or low-CCDC78 expression. E: OS curves for KIRC patients stratified by high- or low-CCDC78 expression. Note: CCDC78, Coiled-coil domain containing 78; ACC, Adrenocortical Carcinoma; BLCA, Bladder Urothelial Carcinoma; COAD, Colon Adenocarcinoma; KIRC, Kidney Renal Clear Cell Carcinoma; OS, Overall Survival; CI, Confidence Interval.

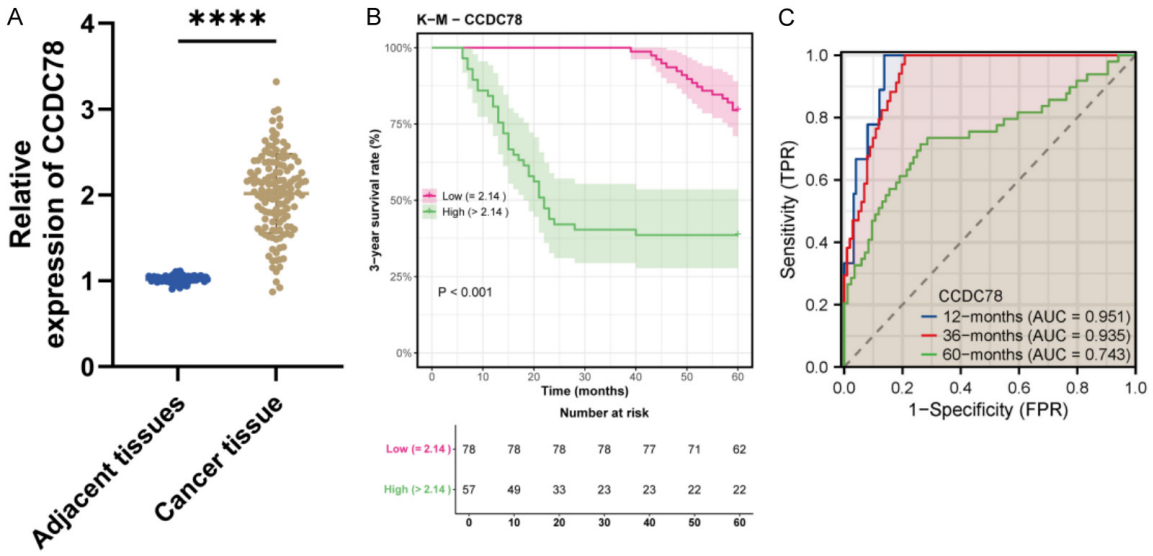


**Figure 3.** CCDC78 expression in CRC tissues and 5-year survival association. A: CCDC78 expression levels in CRC and adjacent normal tissues detected by qRT-PCR. B: 5-year survival curves for high- and low-CCDC78 expression groups. C: Time-dependent ROC curves for CCDC78 in predicting patient prognosis at 12, 36, and 60 months. Note: CCDC78, Coiled-coil domain containing 78; qRT-PCR, Quantitative Real-Time Polymerase Chain Reaction; ROC, Receiver Operating Characteristic.

CCDC78 expression compared to those ≤65 years (P<0.001, **Figure 4A**). TNM staging analysis demonstrated significantly elevated CCDC78 expression in patients with advanced TNM stage (III+IV) compared to those in early-stage (I+II) (P<0.01, **Figure 4C**). Patients with lymph node or distant metastasis exhibited significantly higher CCDC78 expression versus those without metastasis (P<0.05, **Figure 4D**, **4E**). However, no significant difference in CCDC78 expression was detected between poorly differentiated and moderately to well-differentiated tumors (P>0.05, **Figure 4B**). These findings further support the role of CCDC78 as a potential indicator of CRC invasiveness and disease progression.

*CCDC78 as an independent prognostic factor in CRC*

Univariate Cox regression identified age (P< 0.001), tumor differentiation (P=0.002), TNM staging (P<0.001), and CCDC78 expression (P<0.001) as factors significantly associated with CRC prognosis, while gender, perineural invasion, tumor diameter, anatomical location, KRAS mutation, P53 mutation, and Ki67 proliferation index were not (P>0.05). Multivariate Cox regression confirmed age (P=0.012), TNM staging (P<0.001), and CCDC78 expression (P=0.017) as independent CRC prognostic factors, whereas tumor differentiation lost statistical significance after adjustment for other variables (P>0.05) (**Table 2**).

Similarly, TCGA-based univariate Cox regression identified age (P<0.001), pathological T stage (P=0.004), and CCDC78 expression (P<0.001) as significant prognostic factors, while gender and body mass index (BMI) showed no significant association (P>0.05). Multivariate Cox regression further confirmed age (P<0.001), pathological T stage (P=0.007), and CCDC78 expression (P=0.003) as independent prognostic factors (**Table 3**). These results collectively demonstrate that elevated CCDC78 expression is consistently associated with poorer prognosis in both clinical and TCGA datasets and remains an independent prognostic factor after adjustment for confounding variables, suggesting its potential as a CRC prognostic biomarker.

*Prognostic significance of CCDC78 across clinical subgroups*

The prognostic value of CCDC78 was further evaluated in subgroups stratified by age and TNM stage, with patients divided into high- and low-expression groups using a 2.14 cutoff

**Table 1.** Association of CCDC78 expression levels with clinicopathological features in CRC patients

| Variable | Total | CCDC78 Expression Level | | Chi-Square Value | *P*-Value |
|---|---|---|---|---|---|
| | | High (n=57) | Low (n=78) | | |
| Age | | | | | |
| >65 years | 55 (40.74%) | 40 (70.18%) | 15 (19.23%) | 33.325 | <0.001 |
| ≤65 years | 80 (59.26%) | 17 (29.82%) | 63 (80.77%) | | |
| Gender | | | | | |
| Male | 91 (67.41%) | 43 (75.44%) | 48 (61.54%) | 2.298 | 0.130 |
| Female | 44 (32.59%) | 14 (24.56%) | 30 (38.46%) | | |
| Differentiation | | | | | |
| Poorly Differentiated | 21 (15.56%) | 14 (24.56%) | 7 (8.97%) | 4.962 | 0.026 |
| Moderately/Well Differentiated | 114 (84.44%) | 43 (75.44%) | 71 (91.03%) | | |
| TNM Stage | | | | | |
| I-II | 69 (51.11%) | 39 (68.42%) | 30 (38.46%) | 10.661 | 0.001 |
| III-IV | 66 (48.89%) | 18 (31.58%) | 48 (61.54%) | | |
| Perineural Invasion | | | | | |
| Yes | 59 (43.70%) | 26 (45.61%) | 33 (42.31%) | 0.043 | 0.836 |
| No | 76 (56.30%) | 31 (54.39%) | 45 (57.69%) | | |
| Tumor Diameter | | | | | |
| >4 cm | 70 (51.85%) | 32 (56.14%) | 38 (48.72%) | 0.460 | 0.498 |
| ≤4 cm | 65 (48.15%) | 25 (43.86%) | 40 (51.28%) | | |
| Tumor Location | | | | | |
| Left Colon | 18 (13.33%) | 8 (14.04%) | 10 (12.82%) | 0.557 | 0.757 |
| Right Colon | 41 (30.37%) | 19 (33.33%) | 22 (28.21%) | | |
| Sigmoid Colon/Rectum | 76 (56.30%) | 30 (52.63%) | 46 (58.97%) | | |
| Lymph Node Metastasis | | | | | |
| Yes | 63 (46.67%) | 35 (61.40%) | 28 (35.90%) | 7.614 | 0.006 |
| No | 72 (53.33%) | 22 (38.60%) | 50 (64.10%) | | |
| Distant Metastasis | | | | | |
| Yes | 16 (11.85%) | 13 (22.81%) | 3 (3.85%) | 11.333 | 0.001 |
| No | 119 (88.15%) | 44 (77.19%) | 75 (96.15%) | | |
| KRAS Mutation | | | | | |
| Yes | 31 (22.96%) | 15 (26.32%) | 16 (20.51%) | 0.342 | 0.559 |
| No | 104 (77.04%) | 42 (73.68%) | 62 (79.49%) | | |
| P53 Mutation | | | | | |
| Yes | 81 (60.00%) | 37 (64.91%) | 44 (56.41%) | 0.669 | 0.413 |
| No | 54 (40.00%) | 20 (35.09%) | 34 (43.59%) | | |
| Ki67 Proliferation Index | | | | | |
| >60% | 105 (77.78%) | 49 (85.96%) | 56 (71.79%) | 3.050 | 0.081 |
| ≤60% | 30 (22.22%) | 8 (14.04%) | 22 (28.21%) | | |

Note: CCDC78, Coiled-coil domain containing 78; TNM, Tumor Node Metastasis; KRAS, Kirsten rat sarcoma viral oncogene homolog; P53, Tumor protein 53; Ki67, Proliferation marker protein Ki-67.

value. In the age-stratified analysis, patients >65 years with high CCDC78 expression had significantly poorer prognosis compared to those with low expression (P=0.029, **Figure 5A**), and this prognostic difference was more pronounced in patients ≤65 years (P<0.001, **Figure 5B**).

Similarly, TNM stage subgroup analysis showed stage III+IV patients with high CCDC78 expression was associated with significantly worse survival (P=0.024, **Figure 5C**), with similar trends in stage I+II patients (P<0.001, **Figure 5D**). These findings indicate that high CCDC78 expression is consistently associated with

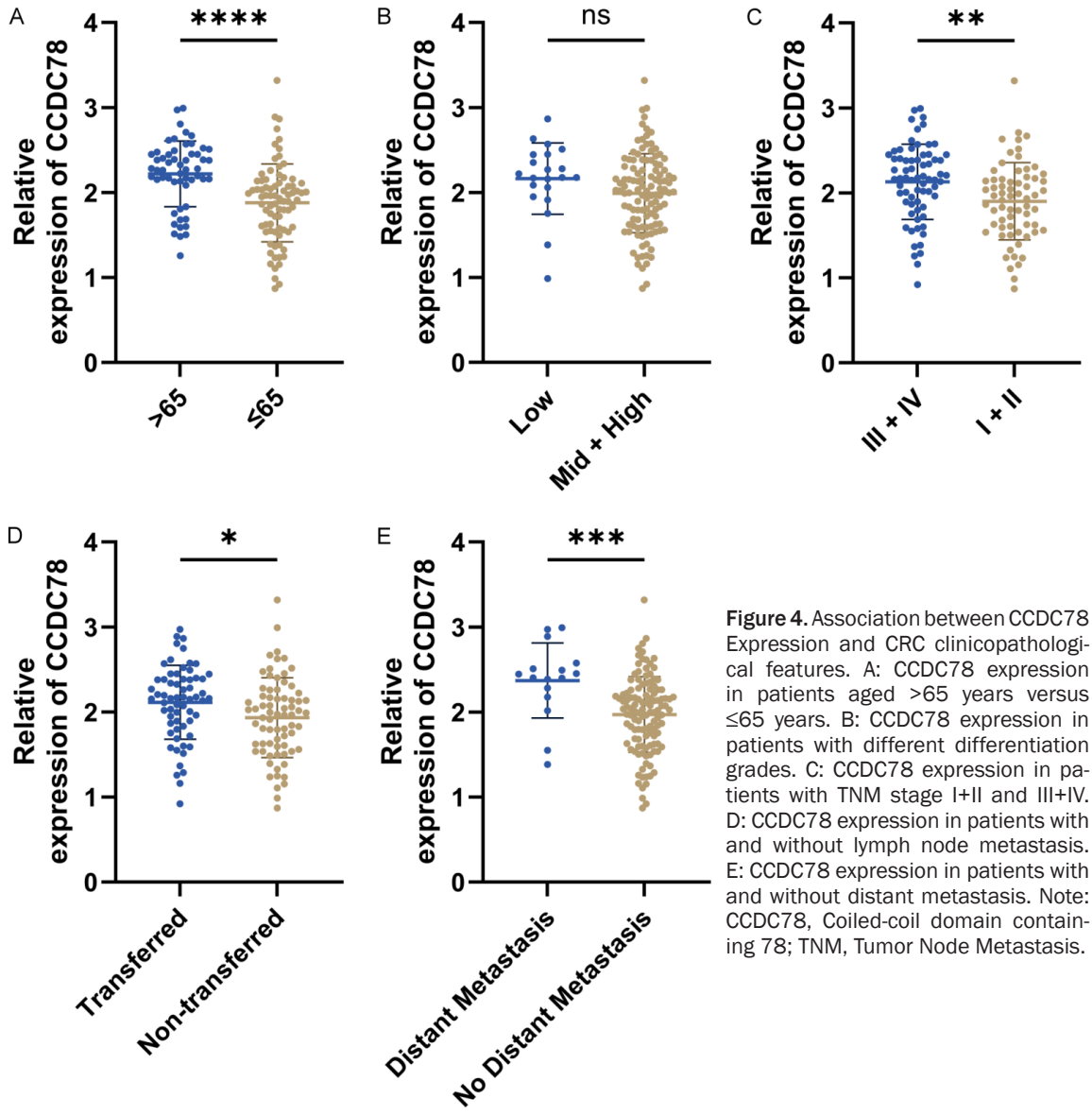


**Figure 4.** Association between CCDC78 Expression and CRC clinicopathological features. A: CCDC78 expression in patients aged >65 years versus ≤65 years. B: CCDC78 expression in patients with different differentiation grades. C: CCDC78 expression in patients with TNM stage I+II and III+IV. D: CCDC78 expression in patients with and without lymph node metastasis. E: CCDC78 expression in patients with and without distant metastasis. Note: CCDC78, Coiled-coil domain containing 78; TNM, Tumor Node Metastasis.

worse prognosis across different age and TNM stage subgroups, reinforcing its potential as a robust CRC prognostic marker.

*Interaction analysis of CCDC78 with prognostic variables*

Interactions between CCDC78 expression and key CRC prognostic variables (age, tumor differentiation, TNM staging) were examined using regression models. Among patients >65 years, high CCDC78 expression (cutoff: 2.14) was associated with a 3.51-fold increased mortality risk (P=0.038, **Figure 6A**), whereas in patients ≤65 years, the risk was markedly higher at 8.37-fold (P=0.004). In the differentiation subgroup, high CCDC78 expression conferred a 4.15-fold increased risk in highly/moderately differentiated tumors (P=0.005, **Figure 6B**), and a 15.06-fold risk in poorly differentiated tumors (P=0.025). TNM stage subgroup analysis associated high CCDC78 expression with significantly elevated risk in stage I+II patients (P<0.001, **Figure 6C**), but no significant effects was observed in stage III+IV patients (P=0.072). These results suggest that the prognostic impact of CCDC78 is particularly pronounced in younger patients, poorly differentiated tumors, and early-stage CRC, highlighting its potential as prognostic biomarker.

**Table 2.** Univariate and multivariate cox regression analysis of crc prognosis based on clinical data

| Variable | Univariate | | | Multivariate | | |
|---|---|---|---|---|---|---|
| | β | *P* Value | HR (95% CI) | β | *P* Value | HR (95% CI) |
| Age | | | | | | |
| >65 years | | | | | | |
| ≤65 years | -1.678 | <0.001 | 0.187 (0.102-0.343) | -0.887 | 0.012 | 0.412 (0.205-0.826) |
| Gender | | | | | | |
| Male | | | | | | |
| Female | 0.295 | 0.304 | 1.343 (0.765-2.358) | | | |
| Differentiation | | | | | | |
| Poorly Differentiated | | | | | | |
| Moderately/Well Differentiated | -0.956 | 0.002 | 0.384 (0.207-0.712) | -0.343 | 0.284 | 0.709 (0.379-1.329) |
| Perineural Invasion | | | | | | |
| Yes | | | | | | |
| No | 0.144 | 0.614 | 1.154 (0.661-2.017) | | | |
| Tumor Diameter | | | | | | |
| >4 cm | | | | | | |
| ≤4 cm | -0.089 | 0.750 | 0.914 (0.528-1.585) | | | |
| Tumor Location | | | | | | |
| Left Colon | | | | | | |
| Right Colon | 0.366 | 0.475 | 1.442 (0.528-3.936) | | | |
| Sigmoid Colon/Rectum | 0.403 | 0.405 | 1.496 (0.58-3.855) | | | |
| TNM Stage | | | | | | |
| I-II | | | | | | |
| III-IV | -2.323 | <0.001 | 0.098 (0.042-0.231) | -1.886 | <0.001 | 0.152 (0.063-0.365) |
| KRAS Mutation | | | | | | |
| Yes | | | | | | |
| No | -0.459 | 0.135 | 0.632 (0.346-1.154) | | | |
| P53 Mutation | | | | | | |
| Yes | | | | | | |
| No | -0.124 | 0.670 | 0.884 (0.501-1.559) | | | |
| Ki67 Proliferation Index | | | | | | |
| >60% | | | | | | |
| ≤60% | -0.207 | 0.557 | 0.813 (0.407-1.623) | | | |
| CCDC78 | | | | | | |
| ≥2.14 | | | | | | |
| <2.14 | -1.646 | <0.001 | 0.193 (0.106-0.35) | -0.84 | 0.017 | 0.432 (0.216-0.863) |

Note: CCDC78, Coiled-coil domain containing 78; TNM, Tumor Node Metastasis; KRAS, Kirsten rat sarcoma viral oncogene homolog; P53, Tumor protein 53; Ki67, Proliferation marker protein Ki-67; HR, Hazard Ratio; CI, Confidence Interval; BMI, Body Mass Index.

*Correlation between CCDC78 and immune cell types*

The relationship between CCDC78 expression and immune cell infiltration in CRC tissues was analyzed across 23 immune cell types. CCDC78 expression significantly correlated with 11 immune cell types (P<0.05, **Figure 7A**). Negative correlations were identified between CCDC78 expression and eosinophils (r=-0.158, P<0.001, **Figure 7B**), immature dendritic cells (iDC, r=-0.092, P=0.019, **Figure 7C**), macrophages (r=-0.158, P<0.001, **Figure 7D**), mast cells (r=-0.180, P<0.001, **Figure 7E**), neutrophils (r=-0.105, P=0.008, **Figure 7F**), T helper cells (r=-0.132, P=0.001, **Figure 7G**), central memory T cells (Tcm, r=-0.138, P<0.001, **Figure 7H**), follicular helper T cells (TFH,

**Table 3.** Univariate and multivariate cox regression analysis of and CRC prognosis based on TCGA data

| Characteristics | Total (N) | Univariate | | Multivariate | |
|---|---|---|---|---|---|
| | | HR (95% CI) | *P* value | HR (95% CI) | *P* value |
| Age | 643 | | | | |
| ≤65 | 276 | Reference | | Reference | |
| >65 | 367 | 1.939 (1.320-2.849) | <0.001 | 1.974 (1.331-2.926) | <0.001 |
| Gender | 643 | | | | |
| Female | 301 | Reference | | | |
| Male | 342 | 1.054 (0.744-1.491) | 0.769 | | |
| BMI | 329 | | | | |
| ≤25 | 107 | Reference | | | |
| >25 | 222 | 0.649 (0.394-1.069) | 0.090 | | |
| Pathologic T stage | 640 | | | | |
| T1-T2 | 131 | Reference | | Reference | |
| T3-T4 | 509 | 2.468 (1.327-4.589) | 0.004 | 2.343 (1.257-4.367) | 0.007 |
| CCDC78 | 643 | 1.343 (1.127-1.601) | <0.001 | 1.303 (1.093-1.553) | 0.003 |

Note: CCDC78, Coiled-coil domain containing 78; BMI, Body Mass Index.

r=-0.102, P=0.010, **Figure 7I**), γδ T cells (Tgd, r=-0.142, P<0.001, **Figure 7J**), and Th2 cells (r=-0.164, P<0.001, **Figure 7K**), suggesting that elevated CCDC78 expression may may be associated with reduced activity or infiltration of these immune cells. Conversely, CCDC78 expression was positively correlated with natural killer (NK) CD56 bright cells (r=0.189, P<0.001, **Figure 7L**), indicating high CCDC78 expression may enhance the activity or recruitment of this NK cell subset. Overall, these findings suggest that CCDC78 may contribute to CRC progression through immune microenvironment modulation.

*GSEA analysis of CCDC78-associated pathways in CRC*

GSEA was performed to identify signaling pathways potentially associated with CCDC78 in CRC and to elucidate its role in tumorigenesis and progression. GSEA identified five significantly enriched signaling pathways associated with high CCDC78 expression (P<0.05, false discovery rate [FDR] q-value <0.441).

The most strongly enriched pathways were the type I interferon-Janus kinase-signal transducer and activator of transcription (JAK-STAT) signaling pathway (set size =21, normalized enrichment score [NES]=1.825, P<0.001, q= 0.044) and the variant mutation-induced retrograde axonal transport pathway (set size =27, NES=1.783, P<0.001, q=0.040). Additional significantly enriched pathways included the RIG-I-NFκB signaling pathway (set size =18, NES= 1.761, P=0.001, q=0.039), WNT signaling modulation via WNT inhibitor (set size =25, NES=1.597, P=0.003, q=0.175), and the G protein-coupled receptor (GPCR)-phospholipase C beta (PLCB)-inositol 1,4,5-trisphosphate receptor (ITPR) signaling pathway (set size =49, NES=1.457, P=0.011, q=0.441).

Among these, the type I interferon-JAK-STAT signaling pathway and retrograde axonal transport pathway exhibited the highest enrichment scores with statistical significance (q<0.05), suggesting that CCDC78 may promote CRC progression through interferon-mediated immune signaling and cytoskeletal transport regulation. Enrichment of RIG-I/NFκB and WNT modulation pathways indicates potential CCDC78 involvement in inflammatory responses and WNT signaling inhibition, while enrichment of the GPCR-PLCB-ITPR pathway further supports potential regulation of the tumor microenvironment via GPCR-mediated signaling. Collectively, these findings suggest that CCDC78 may contribute to CRC progression by regulating immune signaling, cytoskeletal transport, and WNT-related pathways (**Figure 8**).

*CCDC78 expression in cell line models*

CCDC78 expression levels were examined in colorectal cancer cell lines and normal colonic epithelial cells. qRT-PCR demonstrated significantly higher CCDC78 expression in HCT-116

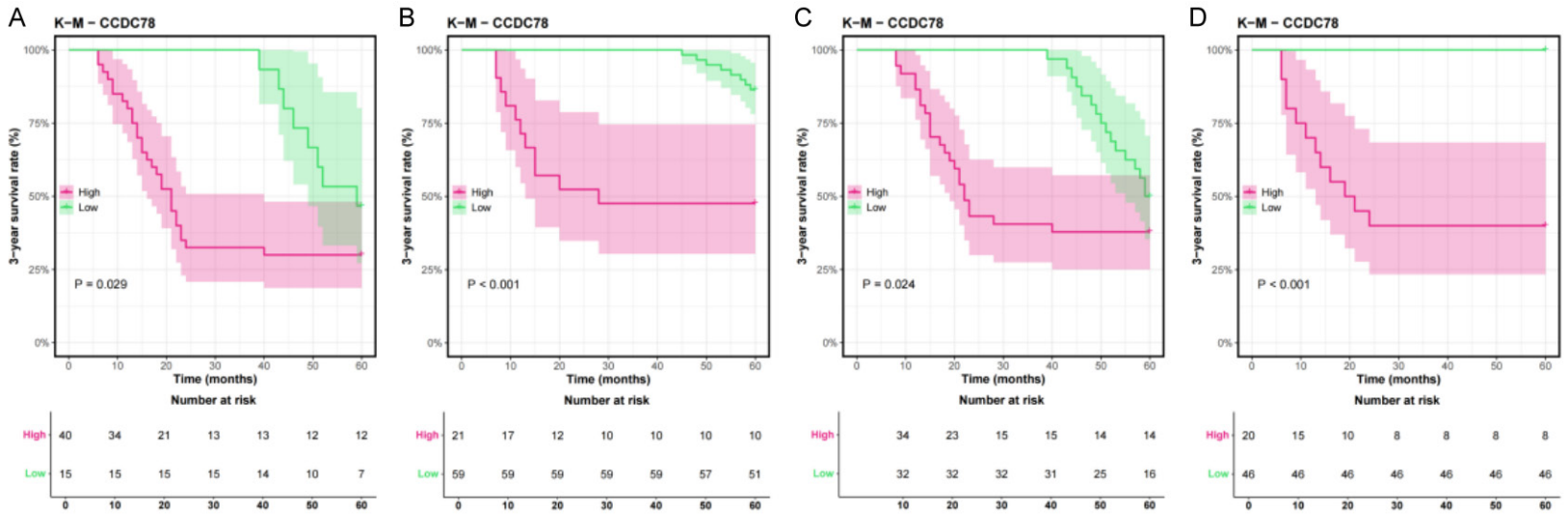


**Figure 5.** Survival analysis of CRC patients with high- or low-CCDC78 expression across clinical subgroups. A: Survival curves for high- and low-CCDC78 expression groups in patients aged >65 years. B: Survival curves for high- and low-CCDC78 expression groups in patients aged ≤65 years. C: Survival curves for high- and low-CCDC78 expression groups in TNM stage III+IV patients. D: Survival curves for high- and low-CCDC78 expression groups in TNM stage I+II patients. Note: CCDC78, Coiled-coil domain containing 78; TNM, Tumor Node Metastasis.

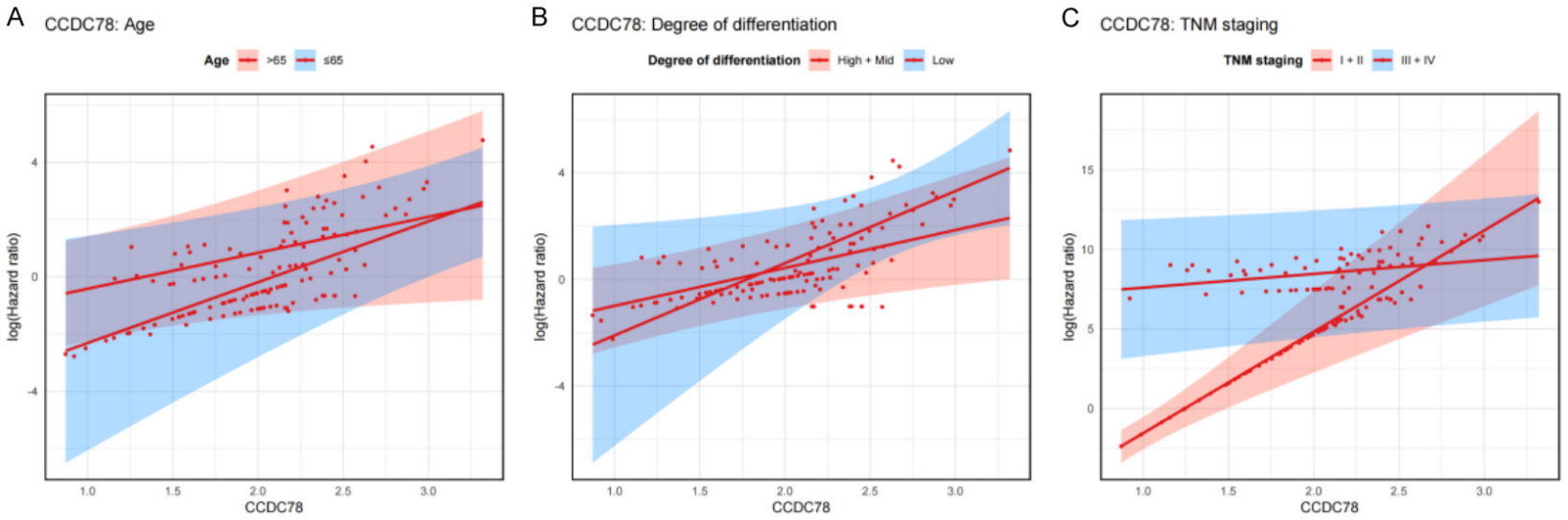

**Figure 6.** Interaction analysis of CCDC78 with clinical variables (Age, Differentiation, TNM Stage). A: Regression curve for the interaction between CCDC78 and age (>65 years vs. ≤65 years). B: Regression curve for the interaction between CCDC78 and differentiation (high/moderate vs. poor). C: Regression curve for the interaction between CCDC78 and TNM stage (I+II vs. III+IV). Note: CCDC78, Coiled-coil domain containing 78; TNM, Tumor Node Metastasis.

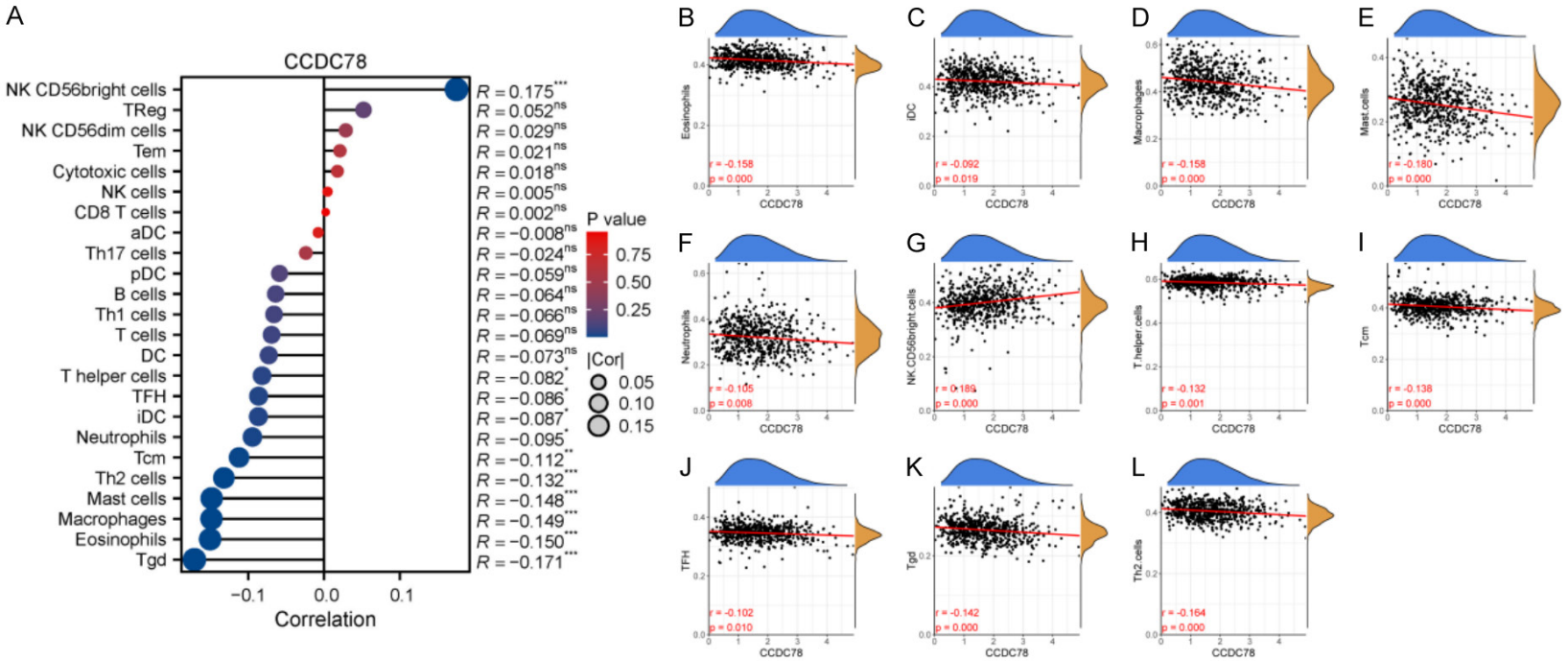


**Figure 7.** Correlation between CCDC78 and immune cell types in CRC tissues. A: Lollipop plot of the correlations between CCDC78 and 23 immune cell types. B: Scatter plot of the correlations between CCDC78 and eosinophils. C: Scatter plot of the correlations between CCDC78 and immature dendritic cells (iDCs). D: Scatter plot of the correlations between CCDC78 and macrophages. E: Scatter plot of the correlations between CCDC78 and mast cells. F: Scatter plot of the correlations between CCDC78 and neutrophils. G: Scatter plot of the correlations between CCDC78 and NK CD56 bright cells. H: Scatter plot of the correlations between CCDC78 and T helper cells. I: Scatter plot of the correlations between CCDC78 and central memory T cells (Tcm). J: Scatter plot of the correlations between CCDC78 and follicular helper T cells (TFH). K: Scatter plot of the correlations between CCDC78 and γδ T cells (Tgd). L: Scatter plot of the correlations between CCDC78 and Th2 cells. Note: CCDC78, Coiled-coil domain containing 78.

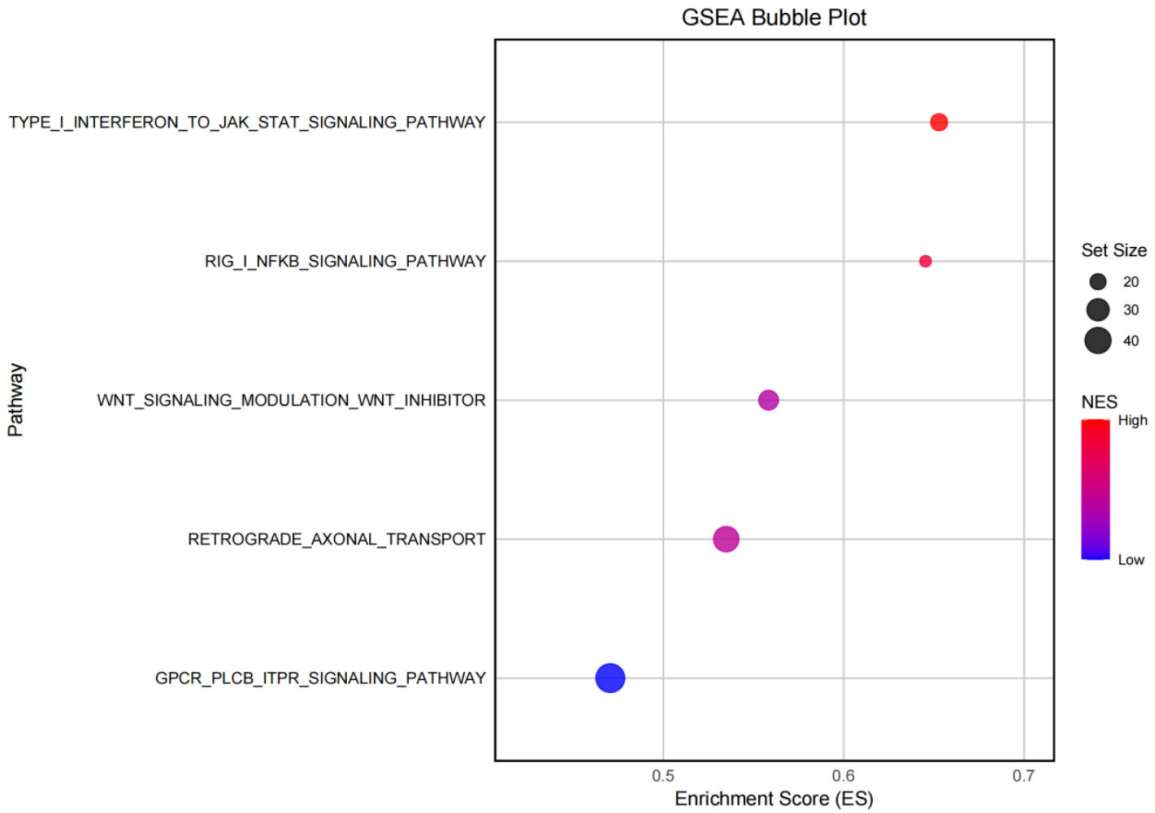


**Figure 8.** GSEA analysis of CCDC78-associated pathways in CRC. Note: GSEA, Gene Set Enrichment Analysis; CCDC78, Coiled-coil domain containing 78.

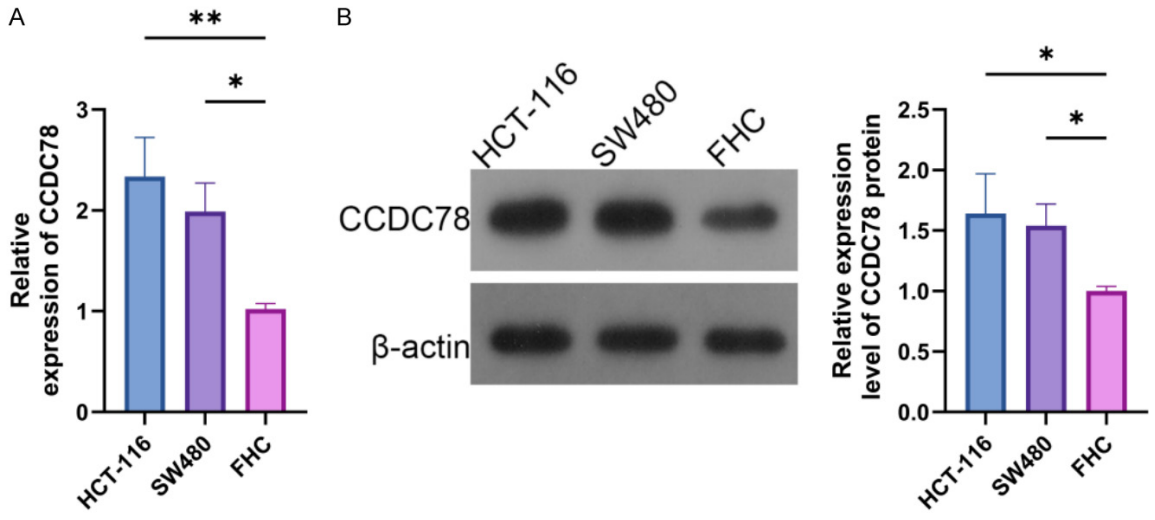


**Figure 9.** CCDC78 expression in different cell lines. A: Relative expression of CCDC78 in different cell lines detected by qRT-PCR. B: Western Blot analysis of the relative expression levels of CCDC78 protein in different cell lines. Note: qRT-PCR, Quantitative Real-Time Reverse Transcription Polymerase Chain Reaction; WB, Western Blot; β-actin, Beta-actin, used as a housekeeping protein; CCDC78, Coiled-Coil Domain Containing 78.

and SW480 cells compared to FHC cells at the mRNA level ($P<0.01$, **Figure 9A**). Western blot analysis further validated these findings at the protein level ($P<0.05$, **Figure 9B**).

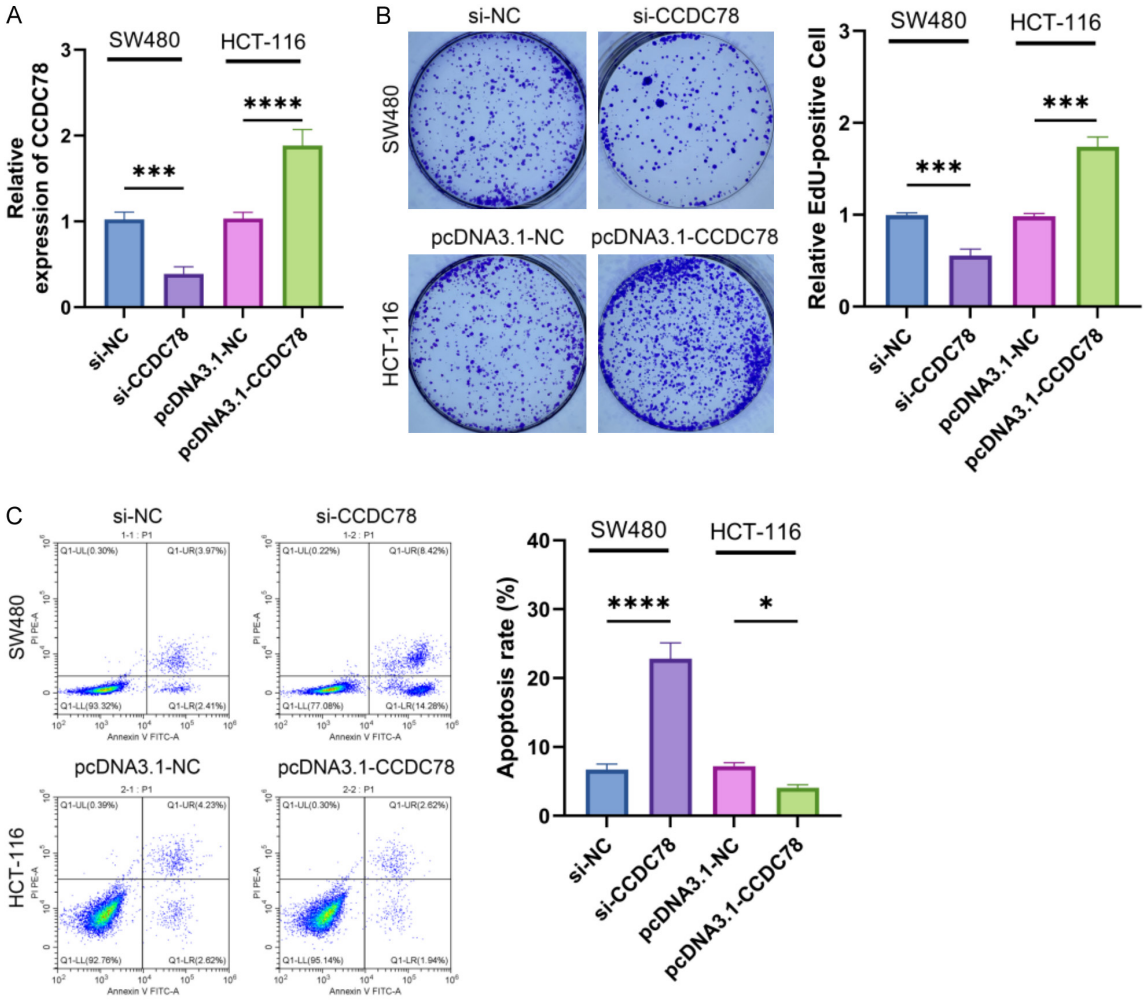


**Figure 10.** The effects of CCDC78 on cell proliferation and apoptosis. A: Relative expression levels of CCDC78 in transfected cells detected by qRT-PCR. B: Effects of CCDC78 expression on cell proliferation in different treatment groups detected by EdU staining. C: Effects of CCDC78 expression on cell apoptosis in different treatment groups detected by Flow cytometry. Note: qRT-PCR, Quantitative Real-Time Reverse Transcription Polymerase Chain Reaction; EdU, 5-Ethynyl-2'-deoxyuridine; CCDC78, Coiled-Coil Domain Containing 78.

*Functional analysis of CCDC78 in transfected cells: expression, proliferation, and apoptosis*

qRT-PCR validated transfection efficiency in HCT-116 cells. CCDC78 mRNA expression was significantly increased in the pcDNA3.1-CCDC78 overexpression group compared to the pcDNA3.1-NC control group (P<0.0001, **Figure 10A**), while expression was markedly reduced in the si-CCDC78 knockdown group relative to the si-NC control group (P<0.001, **Figure 10A**). EdU staining revealed a significant increase in cell proliferation in the pcDNA3.1-CCDC78 group compared to pcDNA3.1-NC group (P<0.001, **Figure 10B**), while si-CCDC78 group demonstrated significantly reduced proliferation relative to si-NC group (P<0.001, **Figure 10B**). Flow cytometry showed that the si-CCDC78 group had significantly higher apoptotic rates than the si-NC group (P<0.0001, **Figure 10C**), while pcDNA3.1-CCDC78 group exhibited significantly lower apoptosis rates versus pcDNA3.1-NC group (P<0.05, **Figure 10C**).

*Effects of CCDC78 transfection on cellular invasion and migration*

Transwell assay demonstrated significantly increased invasion ability in pcDNA3.1-CCDC78 transfected cells compared to pcDNA3.1-NC transfected cells (P<0.01, **Figure 11A**), where-

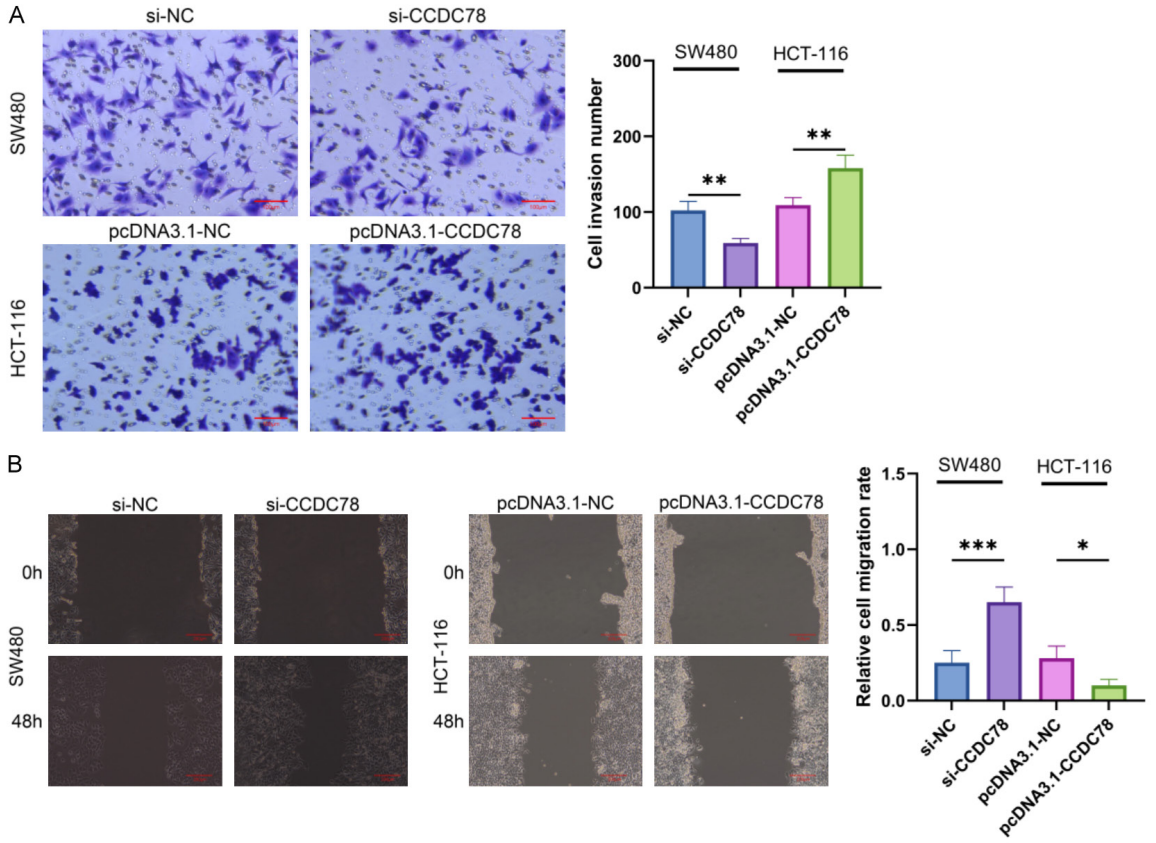


**Figure 11.** The effects of CCDC78 expression on cell invasion and migration. A: Invasion ability of cells assessed by Transwell assay after transfection (×40). B: Migration ability of cells assessed by scratch assay after transfection (×40). Note: CCDC78, Coiled-Coil Domain Containing 78.

as si-CCDC78 group showed significantly reduced invasion ability compared to the si-NC group (P<0.01, **Figure 11A**).

Similarly, wound healing assays showed significantly higher migration rates in the pcDNA3.1-CCDC78 group compared to the pcDNA3.1-NC group (P<0.001, **Figure 11B**), while the si-CCDC78 group demonstrated significantly lower migration rates relative to si-NC group (P<0.05, **Figure 11B**). These results indicate that CCDC78 promotes both invasion and migration in CRC cells.

*CCDC78 regulates JAK-STAT signaling pathway proteins*

Based on GSEA results, the JAK-STAT signaling pathway demonstrated significant enrichment in high CCDC78 expression profiles. Western blot analysis validated pathway activation at protein level. Knockdown of CCDC78 (si-CCDC78 group) significantly reduced the expression of phosphorylated JAK1 (p-JAK1), p-JAK2, p-STAT1, p-STAT3, and CCDC78 in si-CCDC78 group compared with the si-NC group (P<0.0001, **Figure 12**). Conversely, CCDC78 overexpression (pcDNA3.1-CCDC78 group) led to significant upregulation of these phosphorylated proteins compared to control (pcDNA3.1-NC group) (P<0.0001, **Figure 12**). These findings support CCDC78's roles in JAK-STAT signaling pathway modulation.

## Discussion

CRC remains one of the leading causes of cancer-related morbidity and mortality worldwide, with persistently high mortality rates, despite advances in diagnostic and therapeutic technologies [13]. Major clinical challenges, including low early detection rates and poor prognosis in advanced stages, continue to limit effective disease management [14]. CCDC78, a gene involved in cytoskeletal organization and signal transduction, has been suggested to

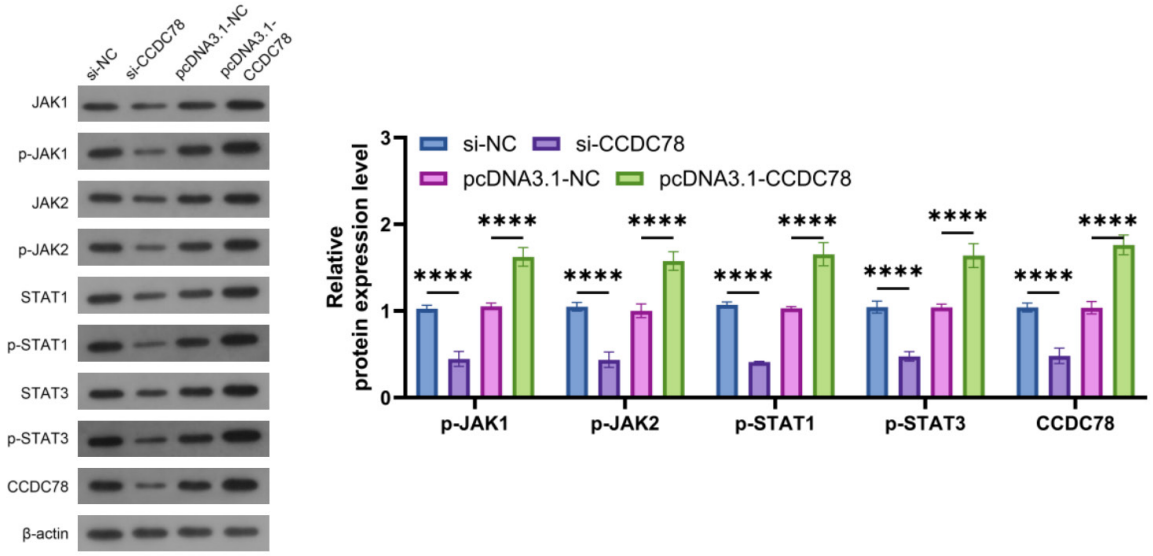


**Figure 12.** The expression of JAK/STAT pathway-related proteins. Note: JAK, Janus Kinase; STAT, Signal Transducer and Activator of Transcription; p-JAK1/p-JAK2/p-STAT1/p-STAT3, Phosphorylated JAK1/JAK2/STAT1/STAT3; CCDC78, Coiled-Coil Domain Containing 78.

regulate tumor cell behavior in preliminary investigations, yet its role in CRC has not been comprehensively characterized. This investigation employed qRT-PCR, TCGA, and GSE30378 datasets to systematically analyze CCDC78 expression profiles, prognostic significance, and associated molecular mechanisms in CRC. The objective was to determine the potential of CCDC78 as a prognostic biomarker and to explore novel targets for precision diagnosis and therapy. The application of comprehensive methodologies has provided multidimensional insights into the role of CCDC78 in CRC progression.

Our findings revealed significantly elevated CCDC78 expression in CRC tumor tissues compared to adjacent non-tumor tissues, suggesting tis pivotal roles in promoting tumor cell proliferation, invasion, and metastasis during CRC initiation and progression. These findings align with previous reports demonstrating high CCDC78 expression in CRC [15]. Similarly, Fan et al. utilized machine learning approaches and reported elevated CCDC78 expression in prostate cancer and several other malignancies [16], indicating potential cancer-type specificity. Mechanistically, CCDC78 overexpression may promote tumor aggressiveness through regulation of cytoskeletal dynamics or intracellular signaling pathways. Supporting this, Lopergolo et al. demonstrated CCDC78 interactions with sarcoplasmic reticulum proteins that influence cytoskeletal regulation in muscle cells [17], while Hong et al. reported its colocalization with microtubules at ciliary tips, emphasizing its role in cytoskeletal organization [18].

Pan-cancer analysis demonstrated that CCDC78 is overexpressed in multiple cancer types, including CRC, ACC, BLCA, and KIRC, with the highest expression observed in CRC. Fan et al. reported that CCDC78 was closely associated with prognosis in castration-resistant prostate cancer (CRPC) [16], while Wu et al. identified CCDC78 as a microtubule-associated marker significantly correlated with survival in diffuse large B-cell lymphoma (DLBCL) [19]. These expression differences may stem from CCDC78's distinct functions in diverse tumor microenvironments, such as cytoskeletal organization or signal transduction roles, which vary by cancer type. In CRC, high CCDC78 expression was significantly associated with reduced five-year survival rates and exhibited high sensitivity and specificity for short- to medium-term prognosis prediction, highlighting its potential utility as an early risk stratification biomarker [15]. However, its long-term prognostic predictive performance declined, possibly due to tumor heterogeneity or therapeutic interventions (e.g., chemotherapy or targeted

therapies) that modulate CCDC78 expression or function. Literature suggests single biomarker predictive power may diminish in long-term follow-up [20], consistent with the observed CCDC78 patterns. Univariate and multivariate Cox regression analyses confirmed CCDC78 as an independent CRC prognostic factor, retaining robustness after adjusting for confounders including age and TNM stage [20]. TCGA data further supported its prognostic value across multiple cancers [16], suggesting CCDC78 may represent a candidate pan-cancer prognostic biomarker.

High CCDC78 expression was significantly associated with advanced age, poor tumor differentiation, advanced TNM staging, lymph node metastasis, and distant metastasis, indicating close association with aggressive tumor biology. For instance, patients with high CCDC78 expression were more likely diagnosed with advanced TNM stages, potentially reflecting its role in promoting tumor progression through pathways related to cell migration or invasion. In contrast, no significant associations were observed with gender, KRAS mutation, or P53 mutation. This pattern suggests CCDC78 may drive tumor invasiveness through specific molecular pathways rather than being directly regulated by common oncogenic mutations. Larger, multicenter studies are warranted to validate these interactions and explore the molecular mechanisms by which CCDC78 contributes to CRC CRC progression in specific clinical subgroups.

Our investigation found CCDC78 expression was negatively correlated with multiple immune cell types, including eosinophils, macrophages, and T helper cells, suggesting it may promote tumor immune evasion by suppressing the infiltration or activity of these cells. Previous reports noted negative correlations between CCDC78 expression and immune cells including macrophages and T helper cells [21]. Additionally, Gao et al. demonstrated that Gab2 influences M2 macrophage polarization, supporting potential immunosuppressive roles for CCDC78 [22]. Conversely, CCDC78 exhibited a positive correlation with NK CD56 bright cells, which are primarily involved in immune regulation. This association may reflect a role for CCDC78 in modulating cytokine secretion and inflammatory signaling, thereby indirectly fostering a pro-tumorigenic microenvironment. These findings highlight the dual regulatory roles of CCDC78 in the CRC immune microenvironment, offering new perspectives on its immunotherapy potential.

GSEA analysis indicated significant enrichment of high CCDC78 expression in several key signaling pathways, including type I interferon-JAK-STAT, RIG-I/NFκB, WNT, and GPCR-PLCB-ITPR signaling pathways. Among these, the most pronounced enrichment was observed in the type I interferon-JAK-STAT pathway, suggesting CCDC78 may promote tumor cell survival by enhancing inflammatory and immune responses, potentially through STAT transcription factor overactivation. Chen et al. reported that CXCL1/miR-302e regulates CRC cell proliferation and metastasis via JAK-STAT pathway [23], while Ghasemian et al. noted that lncRNAs contribute to CRC progression via similar mechanisms [24]. Enrichment of the RIG-I/NFκB pathway suggests that CCDC78 may enhance tumor cell anti-apoptotic capacity by upregulating NFκB downstream anti-apoptotic genes, aligning with evidence that cIAP2/NFκB activation promotes metastasis and chemoresistance in CRC [25]. Furthermore, WNT signaling pathway enrichment indicates a potential role for CCDC78 in regulating tumor cell proliferation and stemness through modulation of WNT inhibitors, potentially linked to aberrant β-catenin activity. This observation is supported by studies implicating β-catenin as a critical mediator of SNTB1-mediated CRC progression [26]. GPCR-PLCB-ITPR pathway activation further supports CCDC78's roles in reshaping tumor microenvironments via G protein-coupled receptor signaling, potentially affecting calcium flux and cell migration. Moy et al. demonstrated critical roles of ITPR3/Ca2+/RELB axis in CRC liver metastasis [27], while Lee et al. linked low PLCB4 expression to CRC drug resistance and MAPK/vascular endothelial growth factor (VEGF) pathway dysregulation [28]. Collectively, these pathways may act synergistically to enhance CRC invasiveness and metastasis, underscoring CCDC78 as a potential therapeutic target. Future investigations should employ functional experiments, such as RNA interference or CRISPR-mediated knockout, to validate CCDC78's specific roles in these pathways and assess its feasibility as a targeted therapy candidate.

By integrating qRT-PCR, TCGA, and GSE30378 datasets, this study systematically validated CCDC78 expression profiles, prognostic significance, and molecular mechanisms in CRC, addressing a critical literature gap. To our knowledge, this is the first comprehensive investigation to elucidate the role of CCDC78 in CRC [15]. It is also the first demonstrating CCDC78's negative correlation with 11 immune cell types and positive correlation with NK CD56 bright cells, providing novel evidence of its involvement in tumor immune microenvironment. GSEA analysis further clarified CCDC78's associations with key pathways including type I interferon-JAK-STAT and WNT, expanding our understanding of the molecular networks driving CRC progression. Moreover, CCDC78 was validated as an independent prognostic biomarker, providing theoretical support for its application in precision diagnosis and risk stratification in CRC. Its dual roles in immune regulation and signal transduction suggest potential applications in targeted and immunotherapies. These findings not only deepen our understanding of CCDC78's biological significance in CRC but also lay foundations for future clinical translation studies.

This investigation further explored the expression of CCDC78 in different cell lines and its functional impacts. Through qRT-PCR and Western blot analysis, results showed significantly elevated CCDC78 expression in HCT-116 and SW480 cells compared to FHC cells, suggesting thar CCDC78 upregulation may be closely related to in CRC progression. Functional assays revealed that CCDC78 overexpression significantly enhanced cell proliferation, apoptosis, migration, and invasion capabilities, whereas CCDC78 knockdown exerted the opposite effects. Flow cytometry analysis confirmed that CCDC78 overexpression inhibited cell apoptosis, while its inhibition enhanced apoptosis. These results indicate that CCDC78 may play key roles in CRC cell biological behavior. Further analysis showed CCDC78 might regulate tumor invasiveness through JAK-STAT signaling pathways. Western blot results indicated that in CCDC78 overexpression groups, phosphorylation levels of JAK1, JAK2, STAT1, and STAT3 were significantly increased, while in inhibition groups, these levels were significantly decreased. This suggests CCDC78 may promote tumor cell growth and metastasis by activating JAK-STAT signaling pathways. This finding provides new molecular targets for CRC therapy. Therefore, CCDC78 is not only a potential prognostic biomarker for CRC but also a promising molecular target for future targeted therapeutic strategies.

This investigation provides valuable insights into the expression and functional roles of CCDC78 in CRC. Our findings indicate that CCDC78 plays critical roles in cell proliferation, invasion, and immune regulation. While this study presents compelling results, further validation in larger and multicenter cohorts would be beneficial to strengthen findings and confirm CCDC78's clinical applicability as a prognostic biomarker. Additionally, the precise molecular mechanisms through which CCDC78 drives tumor progression and modulates immune responses remain incompletely understood. Future investigations should incorporate more comprehensive functional experiments, including *in vivo* animal models and detailed analysis of CCDC78 interactions with key CRC pathways. Furthermore, exploring relationships between CCDC78 and factors including microsatellite instability (MSI) or tumor mutational burden (TMB) would enhance understanding of its immunotherapy roles and provide important insights into its role in immunotherapy responsiveness. Finally, integrating CCDC78 with other biomarkers, and exploring its therapeutic application will be critical for advancing its clinical utility and guiding precision management of CRC.

## Conclusion

CCDC78 is significantly overexpressed in CRC and strongly associated with poor prognosis, establishing its value as an independent prognostic biomarker. By modulating the immune microenvironment and key signaling pathways, including type I interferon-JAK-STAT and WNT, CCDC78 contributes to tumor progression and offers promising avenues for precision diagnosis and targeted therapeutic development.

## Disclosure of conflict of interest

None.

**Address correspondence to:** Yingchang Cai, Department of Anal and Pelvic Floor Surgery, The Quzhou Affiliated Hospital of Wenzhou Medical

University, Quzhou People's Hospital, No. 100 Minjiang Avenue, Kecheng District, Quzhou 324000, Zhejiang, China. E-mail: cyc0202@126.com

## References

[1] McPhail S, Barclay ME, Johnson SA, Swann R, Alvi R, Barisic A, Bucher O, Creighton N, Denny CA, Dewar RA, Donnelly DW, Dowden JJ, Downie L, Finn N, Gavin AT, Habbous S, Huws DW, May L, McClure CA, Møller B, Musto G, Nilssen Y, Saint-Jacques N, Sarker S, Shack L, Tian X, Thomas RJS, Thomson CS, Wang H, Woods RR, You H and Lyratzopoulos G; ICBP Module 9 Chemotherapy Group. Use of chemotherapy in patients with oesophageal, stomach, colon, rectal, liver, pancreatic, lung, and ovarian cancer: an International Cancer Benchmarking Partnership (ICBP) population-based study. Lancet Oncol 2024; 25: 338-351.

[2] Sung H, Ferlay J, Siegel RL, Laversanne M, Soerjomataram I, Jemal A and Bray F. Global Cancer Statistics 2020: GLOBOCAN estimates of incidence and mortality worldwide for 36 cancers in 185 countries. CA Cancer J Clin 2021; 71: 209-249.

[3] Han B, Zheng R, Zeng H, Wang S, Sun K, Chen R, Li L, Wei W and He J. Cancer incidence and mortality in China, 2022. J Natl Cancer Cent 2024; 4: 47-53.

[4] Ju W, Zheng R, Zhang S, Zeng H, Sun K, Wang S, Chen R, Li L, Wei W and He J. Cancer statistics in Chinese older people, 2022: current burden, time trends, and comparisons with the US, Japan, and the Republic of Korea. Sci China Life Sci 2023; 66: 1079-1091.

[5] Cao W, Qin K, Li F and Chen W. Socioeconomic inequalities in cancer incidence and mortality: an analysis of GLOBOCAN 2022. Chin Med J (Engl) 2024; 137: 1407-1413.

[6] Schmitt M and Greten FR. The inflammatory pathogenesis of colorectal cancer. Nat Rev Immunol 2021; 21: 653-667.

[7] Saadh MJ, Allela OQB, Kareem RA, Baldaniya L, Ballal S, Vashishth R, Parmar M, Sameer HN, Hamad AK, Athab ZH and Adil M. Prognostic gene expression profile of colorectal cancer. Gene 2025; 955: 149433.

[8] Lv X, Li X, Chen S, Zhang G, Li K, Wang Y, Duan M, Zhou F and Liu H. Transcriptional dysregulations of seven non-differentially expressed genes as biomarkers of metastatic colon cancer. Genes (Basel) 2023; 14: 1138.

[9] Cai M, He H, Hong S and Weng J. Synergistic diagnostic value of circulating tumor cells and tumor markers CEA/CA19-9 in colorectal cancer. Scand J Gastroenterol 2023; 58: 54-60.

[10] Mohar NP, Cox EM, Adelizzi E, Moore SA, Mathews KD, Darbro BW and Wallrath LL. The influence of a genetic variant in CCDC78 on LMNA-associated skeletal muscle disease. Int J Mol Sci 2024; 25: 4930.

[11] Majczenko K, Davidson AE, Camelo-Piragua S, Agrawal PB, Manfready RA, Li X, Joshi S, Xu J, Peng W, Beggs AH, Li JZ, Burmeister M and Dowling JJ. Dominant mutation of CCDC78 in a unique congenital myopathy with prominent internal nuclei and atypical cores. Am J Hum Genet 2012; 91: 365-371.

[12] Matsuyama T, Ishikawa T, Takahashi N, Yamada Y, Yasuno M, Kawano T, Uetake H and Goel A. Transcriptomic expression profiling identifies ITGBL1, an epithelial to mesenchymal transition (EMT)-associated gene, is a promising recurrence prediction biomarker in colorectal cancer. Mol Cancer 2019; 18: 19.

[13] Bray F, Laversanne M, Sung H, Ferlay J, Siegel RL, Soerjomataram I and Jemal A. Global cancer statistics 2022: GLOBOCAN estimates of incidence and mortality worldwide for 36 cancers in 185 countries. CA Cancer J Clin 2024; 74: 229-263.

[14] Liu Y and Zheng Z. Understanding the global cancer statistics 2022: growing cancer burden. Sci China Life Sci 2024; 67: 2274-2276.

[15] Jin W, Lu Y, Lu J, Wang Z, Yan Y, Liang B, Qian S, Ni J, Yang Y, Huang S, Han C and Yang H. Identification of cancer-associated fibroblast signature genes for prognostic prediction in colorectal cancer. Front Genet 2025; 16: 1476092.

[16] Fan C, Huang Z, Xu H, Zhang T, Wei H, Gao J, Xu C and Fan C. Machine learning-based identification of co-expressed genes in prostate cancer and CRPC and construction of prognostic models. Sci Rep 2025; 15: 5679.

[17] Lopergolo D, Gallus GN, Pieraccini G, Boscaro F, Berti G, Serni G, Volpi N, Formichi P, Bianchi S, Cassandrini D, Sorrentino V, Rossi D, Santorelli FM, De Stefano N and Malandrini A. CCDC78: unveiling the function of a novel gene associated with hereditary myopathy. Cells 2024; 13: 1504.

[18] Hong J, Lee C, Papoulas O, Pan J, Takagishi M, Manzi N, Dickinson DJ, Horani A, Brody SL, Marcotte E, Park TJ and Wallingford JB. Molecular organization of the distal tip of vertebrate motile cilia. bioRxiv 2025.

[19] Wu W, Liu S, Tian L, Li C, Jiang Y, Wang J, Lv Y, Guo J, Xing D, Zhai Y, Sun H, Li Y, Zhang L, He X, Luo K, Zhan H and Zhao Z. Identification of microtubule-associated biomarkers in diffuse large B-cell lymphoma and prognosis prediction. Front Genet 2023; 13: 1092678.

[20] Tang Z, Wu Y, Sun D, Xue X and Qin L. A novel prognostic immunoscore based on The Cancer Genome Atlas to predict overall survival in colorectal cancer patients. Biosci Rep 2021; 41: BSR20210039.

[21] Ding TT, Zeng CX, Hu LN and Yu MH. Establishment of a prediction model for colorectal cancer immune cell infiltration based on the cancer genome atlas (TCGA) database. Beijing Da Xue Xue Bao Yi Xue Ban 2022; 54: 203-208.
[22] Gao X, Long R, Qin M, Zhu W, Wei L, Dong P, Chen J, Luo J and Feng J. Gab2 promotes the growth of colorectal cancer by regulating the M2 polarization of tumor-associated macrophages. Int J Mol Med 2024; 53: 3.
[23] Chen B, Song L, Nie X, Lin F, Yu Z, Kong W, Qi X and Wang W. CXCL1 regulated by miR-302e is involved in cell viability and motility of colorectal cancer via inhibiting JAK-STAT signaling pathway. Front Oncol 2021; 10: 577229.
[24] Ghasemian A, Omear HA, Mansoori Y, Mansouri P, Deng X, Darbeheshti F, Zarenezhad E, Kohansal M, Pezeshki B, Wang Z and Tang H. Long non-coding RNAs and JAK/STAT signaling pathway regulation in colorectal cancer development. Front Genet 2023; 14: 1297093.
[25] Wang R, Wang Y, Liu X, Liu M, Sun L, Pan X, Hu H, Jiang B, Zou Y, Liu Q, Gong Y, Wang M and Sun G. Anastasis enhances metastasis and chemoresistance of colorectal cancer cells through upregulating cIAP2/NFκB signaling. Cell Death Dis 2023; 14: 388.
[26] Liang Y, Wang B, Chen S, Ye Z, Chai X, Li R, Li X, Kong G, Li Y, Zhang X, Che Z, Xie Q, Lian J, Lin B, Zhang X, Huang X, Huang W, Qiu X and Zeng J. Beta-1 syntrophin (SNTB1) regulates colorectal cancer progression and stemness via regulation of the Wnt/β-catenin signaling pathway. Ann Transl Med 2021; 9: 1016.
[27] Moy RH, Nguyen A, Loo JM, Yamaguchi N, Kajba CM, Santhanam B, Ostendorf BN, Wu YG, Tavazoie S and Tavazoie SF. Functional genetic screen identifies ITPR3/calcium/RELB axis as a driver of colorectal cancer metastatic liver colonization. Dev Cell 2022; 57: 1146-1159, e7.
[28] Lee CC, Lee AW, Wei PL, Liu YS, Chang YJ and Huang CY. In silico analysis to identify miR-1271-5p/PLCB4 (phospholipase C Beta 4) axis mediated oxaliplatin resistance in metastatic colorectal cancer. Sci Rep 2023; 13: 4366.